Physics Letters A 375 (2011) 3200–3204

Contents lists available at ScienceDirect

Physics Letters A

www.elsevier.com/locate/pla

First-principles calculations of the electron dynamics during femtosecond laser pulse train material interactions

C. Wang [a], L. Jiang [a,*], F. Wang [b], X. Li [a], Y.P. Yuan [a], H.L. Tsai [c]

[a] Laser Micro/Nano Fabrication Laboratory, School of Mechanical Engineering, Beijing Institute of Technology, Beijing 100081, China
[b] Department of Applied Physics, Beijing Institute of Technology, Beijing 100081, China
[c] Department of Mechanical and Aerospace Engineering, Missouri University of Science and Technology, Rolla, MO 65409, USA

ARTICLE INFO

Article history:
Received 23 May 2011
Received in revised form 29 June 2011
Accepted 8 July 2011
Available online 18 July 2011
Communicated by R. Wu

Keywords:
TDDFT
Electron dynamics
Laser pulse train

ABSTRACT

This Letter presents first-principles calculations of nonlinear electron–photon interactions in crystalline SiO_2 ablated by a femtosecond pulse train that consists of one or multiple pulses. A real-time and real-space time-dependent density functional method (TDDFT) is applied for the descriptions of electrons dynamics and energy absorption. The effects of power intensity, laser wavelength (frequency) and number of pulses per train on the excited energy and excited electrons are investigated.

1. Introduction

Compared with a long pulse, a femtosecond pulse in some aspects fundamentally changes the laser–material interaction mechanisms. A femtosecond pulse laser can easily achieve very high peak power, which is powerful enough for full ionization of almost any solid material with greatly reduced recast, microcracks, and heat-affected zone. Hence, femtosecond lasers are promising for the micro-/nanoscale fabrication of all types of materials [1–4]. The interaction of femtosecond pulse laser with wide band gap materials especially dielectrics such as transparent materials [3,4] is an active research area which has very significant scientific and engineering merits [5–7]. Laser ablation of a wide band gap material is sometimes called laser-induced breakdown in which the material is first transformed into absorbing plasma with metallic properties and subsequent laser–plasma interaction causes the phase changes of bulk materials. Energy transport within the bulk material during the ablation process can be divided into two stages: (1) the photon energy absorption, mainly through free electrons generation, heating, and electron excitation in a time scale from a few femtoseconds to a few picoseconds and (2) the redistribution of the absorbed energy to lattice leading to material removal in a time scale from a few picoseconds to a few nanoseconds. Building up of free electrons is necessary in order to initialize laser ablation of dielectrics [8]. Once the critical free electron density is created, the transparent material becomes opaque, and the absorbed energy is mainly deposited in a very thin layer within a short period of time, which leads to the ablation of the thin layer. A number of different mechanisms were proposed to describe the generation of free electrons. In femtosecond ablation, avalanche ionization [9], electron impact ionization, and photoionization including multiphoton ionization and/or tunnel ionization [10], are major competing mechanisms for free electron generation. The key parameter which controls the ionization mechanism is the Keldysh parameter $\gamma = \omega\sqrt{2I_P}/F$ [11], where ω is the laser frequency, I_P is the ionization potential and F is the field strength. The multiphoton ionization is expected to dominate when $\gamma \gg 1$, while tunnel ionization dominates when $\gamma \ll 1$.

Recent developments of optical devices make it possible to obtain almost any arbitrary pulse shapes. A large number of studies have been reported regarding pulse shaping and its effects on laser–material interactions [12–23]. For example, using a shaped pulse train, ionization process can be controlled [12]; atoms can be selectively ionized [13]; molecular ground state rotational dynamics can be manipulated [14]; chemical reactions can be controlled [15]; and X-ray line emission from plasmas under the femtosecond pulse can be significantly enhanced [16]. Also, it has been experimentally demonstrated that by using temporally shaped pulse trains, the quality of femtosecond laser microstructuring of dielectrics can be improved [18,24]. In theory, the plasma model is used to investigate the pulse train ablation of fused silica, in which quantum theories is employed to calculate the time and

* Corresponding author. Tel.: +86 010 68914517; fax: +86 010 68914517.
E-mail address: jianglan@bit.edu.cn (L. Jiang).

0375-9601/$ – see front matter
doi:10.1016/j.physleta.2011.07.009

space dependent optical and thermal properties, including the electron heat capacity, electron relaxation time, electron conductivity, reflectivity, and absorption coefficient. The numerical calculation shows that nanoscale constant ablation depth can be achieved by the pulse train technology [17].

Although many studies have been conducted, it remains a significant challenge to fundamentally understand the phenomena associated with complex non-equilibrium and nonlinear processes, especially the dissipation of the absorbed energy and the corresponding phase change mechanisms. For further understanding of laser–material interactions, description of quantum electronic dynamics of many-electron systems is essential, which attracts many active electron theoretical treatments for the laser–material interactions system. Up to now, the time-dependent density-functional theory (TDDFT) appears to be the most feasible theoretical framework to treat the electrons quantum mechanically [25]. TDDFT is used to investigate the electron dynamics not only for isolated atoms and molecules [26–28], but also for clusters [29] and bulk systems [30–33] irradiated by intense ultrashort pulses.

This work employs TDDFT to calculate the generation of electrons and the photon energy absorption of α-SiO_2 under single pulse and a pulse train. Fundamental understanding of electron excitations and dynamics irradiated by shaped pulse trains is critical to control and improve micro-/nanoscale processing of materials.

2. Theory

TDDFT is a reformulation of time dependent quantum mechanics, where the fundamental variable is no longer the many-body wave function but the density. This time-dependent density is determined by solving an auxiliary set of non-interacting Schrödinger equations, the Kohn–Sham equations [25]. To describe the motion of electrons, the time-dependent Kohn–Sham (TDKS) equation for single particle orbitals is applied as follows,

$$i\hbar\frac{\partial}{\partial t}\psi(\vec{r},t) = H_{KS}(\vec{r},t)\psi(\vec{r},t) \tag{1}$$

$$n(\vec{r},t) = \sum_i \left|\psi_i(\vec{r},t)\right|^2 \tag{2}$$

where $n(\vec{r},t)$ is the electron density, $H_{KS}(\vec{r},t)$ is the Kohn–Sham Hamiltonian which is conventional separated in the following way [31],

$$H_{KS}(\vec{r},t) = \frac{1}{2m}\left(\vec{p} + \frac{e}{c}\vec{A}(t)\right)^2 + V_{ion}(\vec{r},t) + V_{Hartree}(\vec{r},t) + V_{xc}(\vec{r},t) \tag{3}$$

where e is an elementary charge, $\vec{A}(t)$ is a time-dependent spatially-uniform vector potential which is related to the external electric field, $V_{ion}(\vec{r},t)$ is the electron–ion potential, $V_{xc}(\vec{r},t)$ is the exchange-correlation potential and $V_{Hartree}(\vec{r},t)$ accounts for the classical electrostatic interaction between the electrons.

$$V_{Hartree}(\vec{r},t) = e^2\int dr'\,\frac{n(\vec{r},t)}{|\vec{r}-\vec{r}'|} \tag{4}$$

The choice of the propagator algorithm is crucial for a time-dependent method. This study employs the enforced time-reversal symmetry (ETRS) [34] method to efficiently describe the propagation of electron wave functions in real time. The time evolution of the wave function for a short period Δt is approximately calculated by

$$\psi(\vec{r},t+\Delta t) = e^{-i\hat{H}_{KS}(t+\Delta t)\frac{\Delta t}{2}}e^{-i\hat{H}_{KS}(t)\frac{\Delta t}{2}}\psi(\vec{r},t) \tag{5}$$

where the Hamiltonian $\hat{H}_{KS}(t+\Delta t)$ at time $t+\Delta t$ is calculated from the orbital estimate

$$\psi'(\vec{r},t+\Delta t) = e^{-i\hat{H}_{KS}(t)\Delta t}\psi(\vec{r},t) \tag{6}$$

The number of excited electrons per unit cell $n_{ex}(t)$ is defined as [30],

$$n_{ex}(t) = \sum_{nn'k}\left(\delta_{nn'} - \left|\langle\phi_{nk}|\psi_{n'k}(t)\rangle\right|^2\right) \tag{7}$$

where k is the Bloch wave number and n is the band index.

The electron distribution in the conduction band is defined by the projection of the time-dependent wave function to the initial particle states in the conduction band [31],

$$N_{ex}(m,k) = \sum_{n'}\left(\left|\langle\phi_{mk}|\psi_{n'k}(T)\rangle\right|^2\right) \tag{8}$$

where m represents the particle states.

3. Results and discussion

In our calculations of silica, an orthorhombic unit cell of α-SiO_2 is considered. Lattice constants in three directions are 9.29 a.u. (x axis), 16.09 a.u. (y axis), 10.21 a.u. (z axis), respectively. The irreducible wedge of the Brillouin zone is presented by 154 k points, which corresponds to sampling the full Brillouin zone by 6^3 k points to represent the Bloch wave functions for the momentum-space integration. Our calculations are based on the density functional theory (DFT) within the adiabatic local density approximation. The Ceperley–Alder exchange-correlation functional is used for the uniform electron gas as parameterized by Perdew and Zunger [35]. Interactions between valence electrons and ions are treated by the norm-conserving pseudopotentials [36] with separable nonlocal operators. The electron wave functions are expanded in a plane-wave basis with an energy cutoff of 37 Ry.

We represent the laser irradiation by subjecting our system to an external alternating electric field parallel to the z axis. The time step of $\Delta t = 0.02$ a.u. is used. In addition, the ion position is frozen in all the calculations.

Fig. 1 shows electric field of the applied laser pulse, excited electron, excitation energy and multipoles as a function of time, in which single laser train burst consisting of two pulses is applied. Each of the pulse is a Gaussian wave packet, 800 nm, 16 fs, as shown in Fig. 1(a). The delay (separation) time between the two pulses within a train is 16 fs. The laser peak power density is 5×10^{14} W/cm^2. Figs. 1(a) and 1(e) show that the signal of the multipoles along z axis follows the laser profile with a 1–2 fs delay. Compared with the multipoles along z axis, there is only slight disturbance along x axis and y axis from Fig. 1(d). It achieves the amplitude at around 8 fs and 24 fs, but in smaller magnitude during the second pulse. This is due to the impact of a potential induced by free electron generations, which weakens the laser field.

Fig. 1(b) shows the number of excited electrons. It changes slightly at the initial stage of the laser pulse where the applied electric field is still weak, but it has an abrupt change after 4 fs. This abrupt change is considered a sign of the optical breakdown. Then it reaches the first saturation value at around 12 fs during the first pulse and the next saturation value at around 28 fs during the second pulse. The total energy absorbed from the laser field by the system exhibits the same pattern as the number of excited electrons, which can be seen from Fig. 1(c). After the laser termination, the total absorbed energy is 618.5 eV for the total calculation system and the average energy per excited electron is 27.4 eV.

This study also investigates the effects of the power density, laser wavelength (frequency) and number of pulses per train on the energy absorption and excited electrons. Fig. 2 shows the two cases at peak power densities of 1×10^{15} W/cm^2 and 5×10^{14} W/cm^2 with the same wavelength of 800 nm. It is obvious that excited electrons and absorbed energy increase as the laser

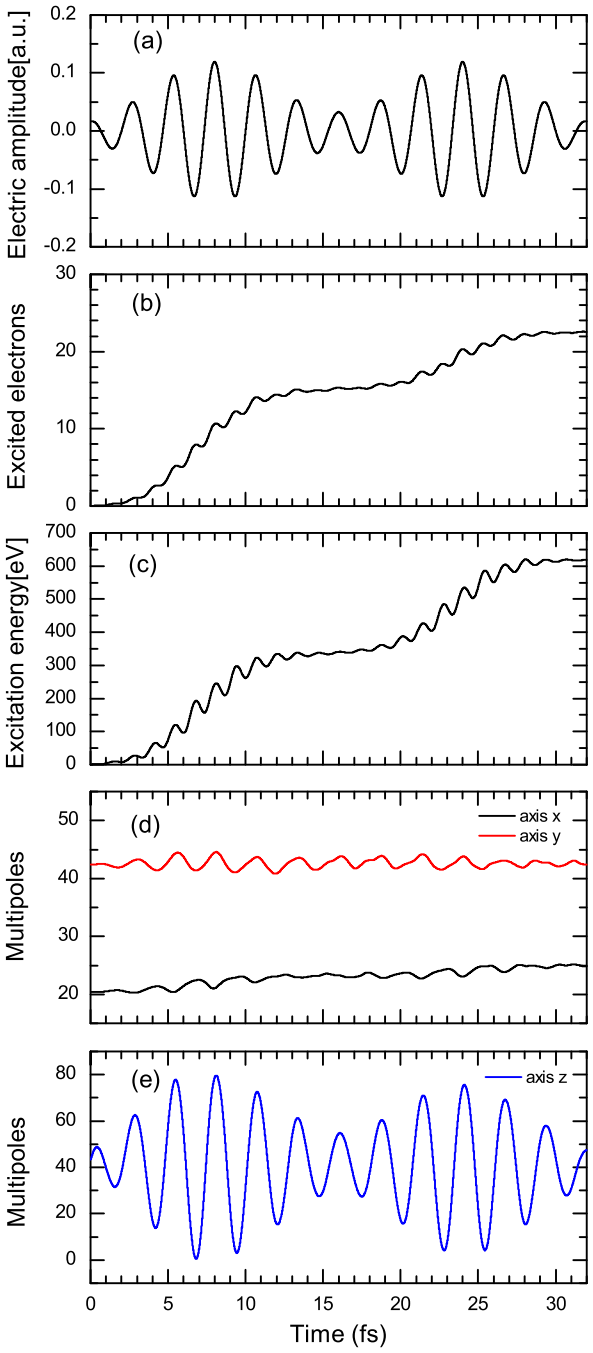

Fig. 1. Electric field of the applied laser pulse, excited electrons, excitation energy and multipoles as a function of time.

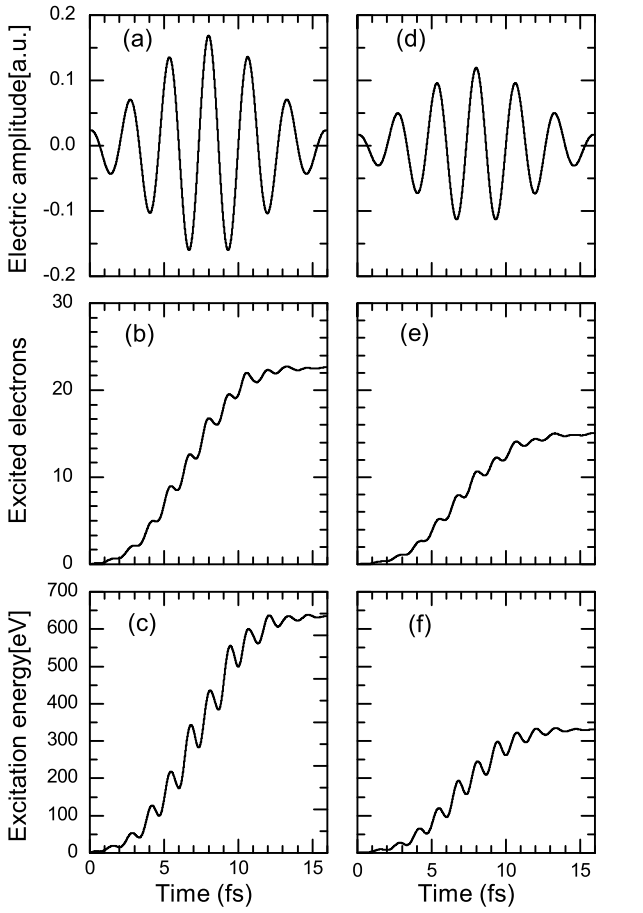

Fig. 2. Electric field of the applied laser pulse, excited electrons and excitation energy as a function of time at various laser intensities. Laser intensity is 1×10^{15} W/cm^2 for the figures on the left. Laser intensity is 5×10^{14} W/cm^2 for the figures on the right. The wavelength is 800 nm.

power density increases. According to Figs. 2(b)–(c) and 2(e)–(f), the average energy absorbed by one electron of these two cases is 28.0 eV and 22.0 eV, respectively. The energy transfer δE and the laser intensity I have a dependence of $\delta E \simeq CI^n$, where n is the number of photons absorbed to free from the valence band [30]. Keldysh theory for solid can also describe the dependence of energy transfer and laser intensity [11]. But these two expressions are only fit in the low intensity region when multiphoton ionization dominates. It remains a challenge to describe the relation between energy transfer and laser intensity when tunnel ionization dominates, which needs further investigations.

Fig. 3 shows the cases of 400 nm and 600 nm laser, with the same peak power density of 5×10^{14} W/cm^2. At the same intensity, energy absorbed from 400 nm and 600 nm laser is more than that from 800 nm laser, which is demonstrated in Figs. 2(f), 3(c) and 3(f). Table 1 shows excitation energies, excited electrons, average absorbed energy per electron after the pulse termination of different lasers with the same power density of 5×10^{14} W/cm^2 and the number of photons absorbed to free from the valence band. The Keldysh parameter γ for these four cases are 0.95 (400 nm), 0.76 (500 nm), 0.64 (600 nm) and 0.48 (800 nm), respectively. This indicates that both tunnel ionization and multiphoton ionization exist in these cases. The number of photons absorbed to free from the valence band can be calculated by $N = [n] + 1$, where $n = E_g/\hbar\omega$, E_g is the band gap of the material, ω is the laser frequency. Due to the well-known underestimation of the band gap energy in the LDA, E_g calculated here is 7 eV. It is found that at the same power density, average absorbed energy per electron is almost inversely proportional to n, that is to say wavelength. This means wavelength is still important for femtosecond laser manipulation of electron dynamics. But for N, the inversely proportional relation is not so apparent, which is due to the tunnel ionization and underestimation of the band gap.

For the case of two pulses per train, the total absorbed energy is 618.5 eV and average energy is 27.4 eV per excited electron, according to Fig. 1(b)–(c), as compared with 635.3 eV and 28.0 eV in Fig. 2(b)–(c) respectively for the case of single pulse with same total energy. The advantages of pulse train are demonstrated. As the ion position is frozen in the calculations, the total absorbed energy is directly split into parts: the first part is converted into the intrinsic thermal excitation energy, and the rest is used for electron emission [29]. When the energy needed to escape from the

Table 1
Excitation energy, excited electrons, average energy absorbed by one electron of various lasers after the laser termination at 5×10^{14} W/cm^2 and the number of photons absorbed to free from the valence band.

Wavelength (frequency)	400 nm (3.10 eV)	500 nm (2.48 eV)	600 nm (2.07 eV)	800 nm (1.55 eV)
Excitation energy/eV	1298.60	1012.36	713.78	331.79
Excited electrons	32.13	29.05	24.33	15.07
Average energy/eV	40.42	34.85	29.34	22.02
$n = E_g/h\omega$	2.26	2.82	3.38	4.52
N-photon ionization	3	3	4	5

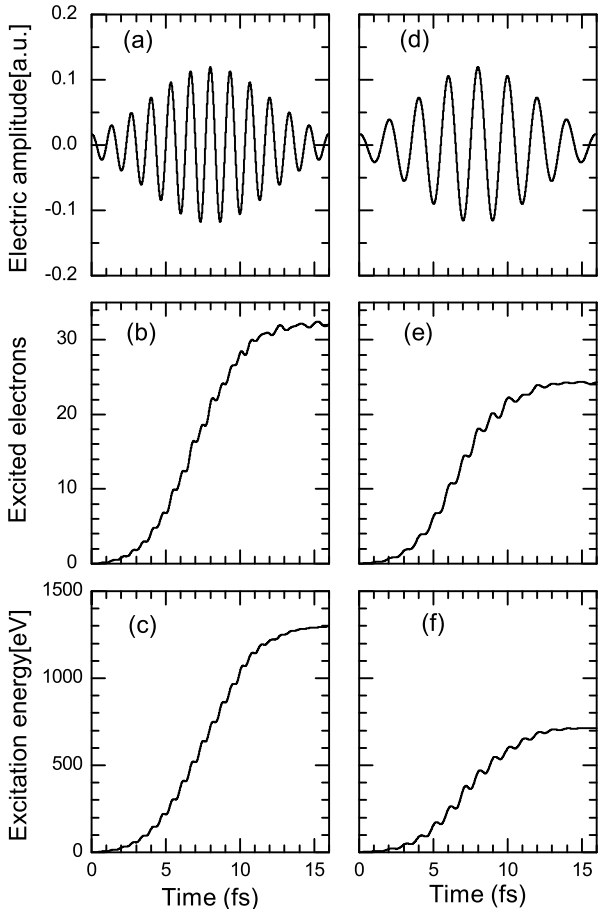

Fig. 3. Electric field of the applied laser pulse, excited electrons and excitation energy as a function of time at various laser wavelengths. Laser wavelength is 400 nm for the figures on the left. Laser wavelength is 600 nm for the figures on the right. The intensity is fixed at 5×10^{14} W/cm^2.

band gap barrier is the same, less energy is converted into the intrinsic excitation energy in the pulse train case. In other word, the highest transient electron temperature is lowered and the energy absorption time is prolonged by pulse train technology, which preserves the advantages of ultrashort lasers, while it can reduce the problems associated with thermal cycles, such as stress-fracturing during laser materials process.

Fig. 4 shows the distribution of the electrons as a function of energy in the conduction band after laser pulse termination. The applied laser intensity (5×10^{14} W/cm^2, 1×10^{15} W/cm^2) is high enough for fully ionization of the material. Therefore, the electrons are broadly distributed between 7–40 eV. On one hand, no obvious differences is observed between 7–20 eV in the three cases. The signals are different in values with the same shapes. On the other hand, electrons distributed between 20–40 eV are 7.60, 3.58 and 7.51, respectively for the three cases, as shown in Fig. 4(a)–(c). Compared with the other two cases, there are more electrons distributed in this zone in the pulse train case. The main reasons

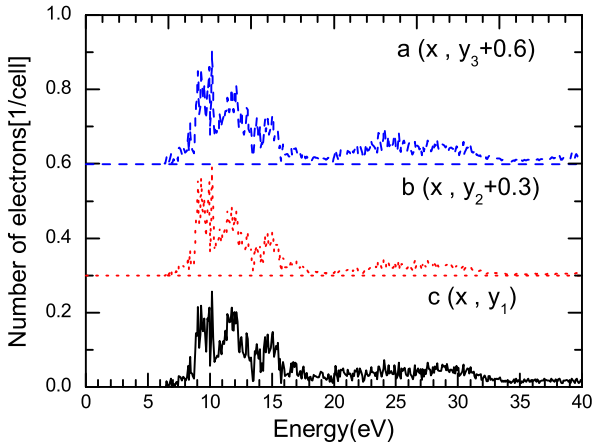

Fig. 4. Occupation of excited electrons in the conduction band after the laser field ends. Each line shows different laser field: (a) two pulses per train at 5×10^{14} W/cm^2 per pulse (blue dashed), (b) single pulse per train at 5×10^{14} W/cm^2 (red dotted), and (c) single pulse per train at 1×10^{15} W/cm^2 (solid). (For interpretation of the references to color in this figure legend, the reader is referred to the web version of this Letter.)

are given as follows: (1) electrons are excited to the conduction band during the first pulse and the distribution of the electrons is changed by the subsequent pulse; (2) the photon absorption time is prolonged by a pulse train, which increases the photon efficiency. However, at such a short time separation (16 fs), the pulses within a train are too close and act like a whole big pulse. Thus, the major advantage of a pulse train cannot be demonstrated completely.

4. Summary

In this Letter, the first-principles calculation for crystalline SiO_2 induced by a femtosecond pulse train is presented, which is supported by the real-time and real-space *ab initio* time-dependent density functional calculations for electrons dynamics and energy absorption. This study investigates the effects of the intensity, the wavelength (frequency) and pulse train on the excited energy and excited electrons. It is demonstrated that: (1) at the same power density, average absorbed energy per electron is almost inversely proportional to wavelength; (2) average energy absorbed by one electron is lower in the pulse train consisting of two pulses case; (3) the pulse train technology prolongs the energy absorption time and prevents overheating of electrons; (4) the distribution of the electrons can be changed by the pulse train technology. Further investigations are required to understand the impacts of other process parameters, such as the number of pulses per train, pulse delay, and pulse intensity distribution by using the first-principles calculations.

Acknowledgements

The authors thank the research group free OCTOPUS code, which is composed by Miguel A.L. Marques, Angel Rubio, and Al-

berto Castro. This research is supported by the National Natural Science Foundation of China (Grant Nos. 90923039 and 51025521) and the 111 Project of China (Grant No. B08043).

References

[1] G. Dumitru, V. Romano, H.P. Weber, M. Sentis, W. Marine, Appl. Phys. A 74 (2001) 729.
[2] L. Jiang, H.L. Tsai, ASME J. Heat Transfer 127 (2005) 1167.
[3] P.P. Pronko, S.K. Dutta, D. Du, R.K. Singh, J. Appl. Phys. 78 (1995) 6233.
[4] M. Lenzner, J. Krüer, S. Sartania, Z. Cheng, C. Spielmann, G. Mourou, W. Kautek, F. Krausz, Phys. Rev. Lett. 80 (1998) 4076.
[5] A. Kaiser, B. Rethfeld, M. Vicanek, G. Simon, Phys. Rev. B 61 (2000) 11437.
[6] F. Ladieu, P. Martin, S. Guizard, Appl. Phys. Lett. 81 (2002) 957.
[7] R. Stoian, D. Ashkenasi, A. Rosenfeld, E.E.B. Campbell, Phys. Rev. B 62 (2000) 13167.
[8] L. Jiang, H.L. Tsai, ASME J. Heat Transfer 128 (2006) 926.
[9] S.S. Mao, F. Quéré, S. Guizard, X. Mao, R.E. Russo, G. Petite, P. Martin, Appl. Phys. A 79 (2004) 1695.
[10] Y.A. Il'insky, L.V. Keldysh, Electromagnetic Response of Material Media, Plenum, New York, 1994.
[11] L.V. Keldysh, Sov. Phys. JETP 20 (1965) 1307.
[12] R. Bartels, S. Backus, E. Zeek, L. Misoguti, G. Vdovin, I.P. Christov, M.M. Murnane, H.C. Kapteyn, Nature 406 (2000) 164.
[13] A. Lindinger, C. Lupulescu, M. Plewicki, F. Vetter, A. Merli, M.S. Weber, L. Wöste, Phys. Rev. Lett. 93 (2004) 033001.
[14] M. Renard, E. Hertz, B. Lavorel, O. Faucher, Phys. Rev. A 69 (2004) 043401.
[15] A. Assion, T. Baumert, M. Bergt, T. Brixner, B. Kiefer, V.V. Seyfried, M. Strehle, G. Gerber, Science 282 (1998) 919.
[16] A.A. Andreev, J. Limpouch, A.B. Iskakov, H. Nakano, Phys. Rev. E 65 (2002) 026403.
[17] L. Jiang, H.L. Tsai, Appl. Phys. Lett. 87 (2005) 151104.
[18] R. Stoian, M. Boyle, A. Thoss, A. Rosenfeld, G. Korn, I.V. Hertel, E.E.B. Campbell, Appl. Phys. Lett. 80 (2002) 353.
[19] M. Spyridaki, E. Koudoumas, P. Tzanetakis, C. Fotakis, R. Stoian, A. Rosenfeld, I.V. Hertel, Appl. Phys. Lett. 83 (2003) 1474.
[20] E. Ohmaru, T. Okamoto, S. Fujiwara, T. Sano, I. Miyamoto, J. Jpn. Soc. Precis. Eng 71 (2005) 284.
[21] M. Lapczyna, K.P. Chen, P.R. Herman, H.W. Tan, R.S. Marjoribanks, Appl. Phys. A 69 (1999) S883.
[22] I.H. Chowdhury, X.F. Xu, A.M. Weiner, Proc. SPIE 4978 (2003) 138.
[23] X. Li, L. Jiang, H.L. Tsai, J. Appl. Phys. 106 (2009) 064906.
[24] R. Stoian, A. Mermillod-Blondin, S. Winkler, A. Rosenfeld, I.V. Hertel, M. Spyridaki, E. Koudoumas, C. Fotakis, I.M. Burakov, N.M. Bulgakova, Proc. SPIE Int. Opt. Eng. 5662 (2004) 593.
[25] M.A.L. Marques, E.K.U. Gross, Annu. Rev. Phys. Chem. 55 (2004) 427.
[26] J.L. Krause, K.J. Schafer, K.C. Kulander, Phys. Rev. A 45 (1992) 4998.
[27] S. Chelkowski, T. Zuo, A.D. Bandrauk, Phys. Rev. A 46 (1992) R5342.
[28] I. Kawata, H. Kono, Y. Fujimura, J. Chem. Phys. 110 (1999) 11152.
[29] F. Calvayrac, P.-G. Reinhard, E. Suraud, C.A. Ullrich, Phys. Rep. 337 (2000) 493.
[30] T. Otobe, M. Yamagiwa, J.-I. Iwata, K. Yabana, T. Nakatsukasa, G.F. Bertsch, Phys. Rev. B 77 (2008) 165104.
[31] T. Otobe, J. Phys.: Condens. Matter 22 (2010) 384204.
[32] T. Otobe, K. Yabana, J.-I. Iwata, J. Phys. 21 (2009) 064224.
[33] Y. Shinohara, K. Yabana, Y. Kawashita, J.-I. Iwata, T. Otobe, G.F. Bertsch, Phys. Rev. B 82 (2010) 155110.
[34] A. Castro, M.A.L. Marques, A. Rubio, J. Chem. Phys. 121 (2004) 3425.
[35] J.P. Perdew, A. Zunger, Phys. Rev. B 23 (1981) 5048.
[36] N. Troullier, J.L. Martins, Phys. Rev. B 43 (1991) 1993.